VOL. 11, NO. 1, JANUARY 2016 ISSN 1819-6608
ARPN Journal of Engineering and Applied Sciences

www.arpnjournals.com

STUDY ON TURBULENT CHARACTERISTICS OF FLOW BOILING IN A MICRO GAP UNDER THE INFLUENCE OF SURFACE ROUGHNESS AND MICRO FINS

Shugata Ahmed[1], Ahmad Faris Ismail[1], Erwin Sulaeman[1] and Muhammad Hasibul Hasan[2]
[1]Departmental of Mechanical Engineering, Faculty of Engineering, Jalan Gombak, Kuala Lumpur, Malaysia
[2]Departmental of Manufacturing and Materials Engineering, Faculty of Engineering, Jalan Gombak, Kuala Lumpur, Malaysia
E-Mail: shugataahmed@gmail.com

ABSTRACT

Micro gap heat sinks with internal micro fins are potential candidates for evaporative cooling of miniature electronic devices. Generation of turbulence during flow boiling in a micro gap is an important issue in two-phase heat transfer analysis. Surface roughness and fins play important role in turbulence generation. In this paper, effects of micro gap height, surface roughness and fin spacing on turbulence generation during flow boiling of pure water in this particular heat sink have been investigated by numerical simulation. Commercial software FLUENT 14.5 release has been used for simulation purpose. Volume of Fluid (VOF) model along with Renormalization Group Theory (RNG) based $k-\varepsilon$ turbulence model has been used for fluid flow and heat transfer modeling. Simulation results demonstrate that turbulent kinetic energy increases in the flow direction due to large pressure drop inside micro gap. As pressure drop decreases with the increment of gap height, turbulent kinetic energy also declines. For the same reason, it has been found that generation of turbulent kinetic energy is lower for larger fin spacing. On the other hand, effect of surface roughness on turbulent kinetic energy is dominated by flow scale. For same Reynolds number, turbulence in larger fluid domains is more sensitive to surface roughness than smaller flow fields.

Keywords: micro gap, surface roughness, micro fin, flow boiling, pressure drop and turbulent kinetic energy.

INTRODUCTION

With the new trend of miniaturization, electronic devices are becoming more compact day by day. On the other hand, speed and functionality of these devices are increasing. As a result, heat dissipation from integrated circuits is on the rise. Hence, thermal management of densely packed electronic devices and microelectromechanical systems (MEMS) has become a cutting edge research area.

Microchannels are considered as a solution of thermal management system of ingrowing power dissipation from digital devices with high gate density. It has high heat dissipation capability resulting from its large heat transfer surface-to-volume ratio. This advantageous characteristic of microchannels was noted first by Tuckerman and Peace [1]. They found that dissipated heat flux from a 60 μm wide and 302 μm deep channel is up to790 Wm^{-2}, while using water as an energy transmission fluid. However, the pressure drop was more than 2 bars and stream wise surface temperature rise was also very high as thermal boundary layer develops in the flow direction. Due to higher pressure drop, higher pumping power is required to drive the fluid through microchannels.

In recent years, various new techniques have been developed for electronic cooling. Evaporative cooling has been found very effective for extensive heat transfer from microelectronic devices. However, flow boiling instabilities such as temperature and pressure fluctuations are major challenges in two-phase heat transfer. Micro gap heat sinks can effectively reduce flow boiling instabilities. The significant beneficial characteristics of micro gaps over microchannels are generation of more uniform surface temperature, decrement of flow boiling instability, lower pressure drop and high heat transfer coefficient [2].

Micro fins can be effectively used with micro gap heat sinks for high performance cooling. Micro fins not only increase surface area but also generate turbulence [3]. Hence, heat transfer rate augments. Figure-1 shows a micro finned micro gap heat sink created by ANSYS Workbench Design Modeler.

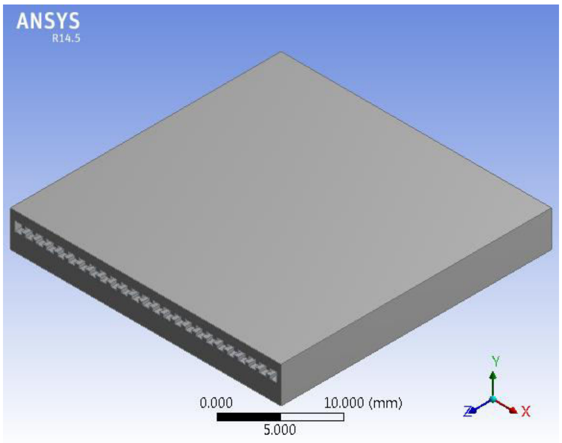

Figure-1. Micro finned micro gap (3D view).

Generally, turbulence is characterized by high Reynolds number. If Reynolds number is higher than transition Reynolds number($\mathrm{Re} > 2400$), the flow is assumed as turbulent. However, researchers have different opinions on transition Reynolds number for microchannels. Nguyen *et al.* [4] noticed flow transition in a trapezoidal microchannel at low Reynolds number.

Surface roughness is one of the major aspects of microchannel fabrication due to its high impact on micro-scale fluid flow and heat transfer. Surface roughness can be originated either in manufacturing stage because of machining process or later due to erosion. Seder et al. [5] investigated effect of various machining processes and parameters on surface finish of microchannels. They showed that spindle speed and tool diameter play important role on surface finish in CNC milling. Again, wire-cut electrical discharge machining (EDM) can generate smoother surfaces than CNC milling. Surface roughness also can be generated due to improper fixation as it may induce vibration during machining. Material properties are also responsible for surface finish quality. Surface roughness of channel walls may result higher pressure drop and generate vortex in the fluid. Wu et al. [6] observed early flow transition for nitrogen gas in rectangular microchannel due to surface roughness.

Study on turbulence modeling for single and two-phase flow has been done by many researchers. Various turbulence models were compared by Mirzabeygi and Zhang [7] to determine appropriate model for simulating two-phase flow in a condenser. By comparing with experimental data, they recommended RNG $\mathrm{k}-\varepsilon$ turbulence model for this purpose. Comparison between various turbulence models for numerical analysis of subcooled boiling in a vertical pipe had been done by Zhang *et al.* [8] they concluded that $\mathrm{k}-\varepsilon$ turbulence models perform better than $\mathrm{k}-\omega$ models for CFD analysis. A correlation between pressure drop and turbulence intensity had been established by Vlahostergios *et al*. [9] Details on turbulence simulation in ANSYS CFX software is given in [10], where authors analyzed erosion rate during turbulent flow in a tunnel. A CFD comprehensive study on generating turbulence in a concentric annular duct to increases heat transfer rate was carried out by Kelvin *et al*. [11]

In this paper, turbulent kinetic energy generation during flow boiling of water in a micro finned micro gap has been investigated numerically. Simulation has been done by commercial CFD analysis software FLUENT 14.5 release. Effects of micro gap height, fin spacing and surface roughness have been considered.

MATHEMATICAL MODELING

Governing equations

A complete mathematical model of the system is necessary for numerical analysis of the heat sink. From Eqn. (1) – (4) are steady-state governing equations for flow boiling and heat transfer, which have been derived from volume of fluid (VOF) model [12]. In VOF model, each phase is considered as a single-fluid. Hence, separate sets of governing equations are used for liquid and vapor phases. These equations have been solved numerically by applying proper boundary conditions.

The continuity equation for vapor phase, which is also known as void fraction equation, is the following:

$$\rho_v \nabla(\alpha.\vec{\boldsymbol{v}}_{\boldsymbol{v}}) = \dot{m}_{l\to v} - \dot{m}_{v\to l} \tag{1}$$

Here ρ_v and $\vec{\boldsymbol{v}}_{\boldsymbol{v}}$are density and velocity of vapor respectively. By solving Eqn. (1), distribution of void fraction is obtained in the flow domain. Later volume fraction distribution of liquid phase is calculated from$1-\alpha$. $\dot{m}_{l\to v}$ and $\dot{m}_{v\to l}$ represent mass transfer from liquid to vapor and vice versa respectively.

For a Newtonian fluid, conservation of momentum equation is given below:

$$\rho\nabla(\vec{\boldsymbol{v}}.\vec{\boldsymbol{v}}) = -\nabla P + \nabla\tau + \rho\vec{\boldsymbol{g}} + \vec{\boldsymbol{F}}_{\boldsymbol{\sigma}} \tag{2}$$

In Eqn. (2), ∇P are $\nabla\tau$ pressure and shear stress gradients respectively, $\vec{\boldsymbol{g}}$ is the gravitational acceleration and $\vec{\boldsymbol{F}}_{\boldsymbol{\sigma}}$ denotes the surface tension force.

Conservation of energy equation for fluid domain is written as:

$$\rho_v\nabla(\alpha.E_v.\vec{\boldsymbol{v}}_{\boldsymbol{v}}) = \nabla\big(k_{eff}\nabla\theta_v\big) + h_{lv}(\dot{m}_{v\to l} - \dot{m}_{l\to v}) \tag{3}$$

Here E_v and θ_v are enthalpy and temperature of vapour respectively, k_{eff} represents effective thermal conductivity and h_{lv} is the enthalpy of vaporization.

For solid domain, the energy equation can be written as:

$$\nabla(k_s\nabla\theta) = 0 \tag{4}$$

Here $C_{p,s}$ and θ are specific heat capacity and temperature of the solid domain respectively.

Mass exchange between two phases is calculated from evaporation-condensation model, proposed by Lee [13]:

$$\dot{m}_{l\to v} = \varepsilon * (1-\alpha)\rho_l \frac{(T_l - T_{sat})}{T_{sat}} \tag{5}$$

$$\dot{m}_{v\to l} = \upsilon * \alpha\rho_v \frac{(T_{sat} - T_v)}{T_{sat}} \tag{6}$$

Here, ε and υ are evaporation and condensation coefficients respectively. Wu et al. [14], De Schepper et al. [15] and Alizadehdakhel *et al.* [16] recommended the value 0.1 of these coefficients to maintain interfacial temperature close to saturation temperature, T_{sat}.

From Eqn. (7) – (8) are governing equations for turbulence, which have been obtained from Renormalization Group Theory (RNG) based $k-\varepsilon$ turbulence model [17]. The equations are stated below:

$$\rho\nabla(\vec{v}.k) = \nabla(a_k.\mu_{eff}.\nabla k) + G_k + G_b - \rho\varepsilon - Y_M + S_k \quad (7)$$

$$\rho\nabla(\vec{v}.\varepsilon) = \nabla(a_\varepsilon.\mu_{eff}.\nabla\varepsilon) + C_{1\varepsilon}\frac{\varepsilon}{k}(G_k + C_{3\varepsilon}G_b) - C_{2\varepsilon}\rho\frac{\varepsilon^2}{k} - R_\varepsilon + S_\varepsilon \quad (8)$$

In above equations, k and ε are turbulent kinetic energy and and rate of energy dissipation respectively.

G_k = generation of turbulent kinetic energy due to the mean velocity gradients

G_b= generation of turbulent kinetic energy due to buoyancy

Y_M= contribution of the fluctuating dilatation in compressible turbulence to the overall dissipation rate.

a_k and a_ε are inverse effective Prandtl numbers for k and ε respectively and S_k and S_ε are source terms.

The model constants have following default values:

$C_{1\varepsilon}$ = 1.42, $C_{2\varepsilon}$ = 1.68.

Boundary conditions

Following boundary conditions are applied in the computational domain:

Inlet: $T_f = T_{in}$, $\dot{m} = \dot{m}_{in}$, $\alpha = 0$. In this study, inlet temperature has been kept constant at 25°C.

Outlet: $P = P_{out}$. Atmospheric pressure is defined at the outlet of the heat sink.

Solid-fluid interface: Heat transfer from wall to fluid by convection, $q_{eff} = h(\theta - \theta_f)$.

Channel bottom wall: Uniform heat flux is applied at the bottom of the heat sink. Heat is transferred through solid wall by conduction in the normal direction of bottom surface, $q = -k_s\frac{\partial\theta}{\partial n}$.

Other channel walls: Other channel walls are considered as insulated. Hence, $\frac{\partial\theta}{\partial n} = 0$.

GEOMETRY, MESHING AND NUMERICAL SOLUTION

The geometry has been generated by ANSYS Workbench Design Modeler. Dimensions of the sink are provided in Table-1. Heat sink material is aluminum. After creating geometry, fine meshing has been done. Number of meshing elements has been optimized to reduce computational time. Fluid flow and heat transfer are assumed as steady-state.

FLUENT uses Finite Volume Method to solve governing equations. Second Order Upwind scheme has been used for spatial discretization of the governing equations. Semi-Implicit Method for Pressure Linked Equations (SIMPLE) algorithm, developed by Patankar and Spalding [18] has been adopted to solve pressure-velocity coupling equation.

Table-1. Dimensions of heat sink, micro gap and fins.

Parameters (unit)	**Value**
Heat sink height, H (mm)	4
Heat sink width, W (mm)	30
Heat sink length, L (mm)	30
Micro gap height (mm)	1
Fin height, H_{fin} (mm) Fin width-to-fin spacing ratio (β)	0.3 0.2-2.174
Number of fins, N	48

RESULTS AND DISCUSSIONS

Effect of micro gap height and fin spacing

From Figure-2., contour plot of pressure and turbulent kinetic energy (k) distribution on X-Z plan for Re = 1100 has been shown. It is perceived that pressure decreases in the flow direction. As a result, turbulent kinetic energy increases due to velocity increment although the flow is laminar.

In Figure-3., contour plot of turbulent kinetic energy distribution on X-Y plan has been shown. It is seen that turbulent kinetic energy is high near fins and channel walls and low in the middle of the gap.

Increment of turbulent kinetic energy during flow through the micro gap is influenced by gap height. In Figure-4., it is observed that k decreases with gap height increment, while mass flow rate, $\dot{m} = 0.059$ kg/s has been maintained. This is because pressure drop inside micro gap is smaller for higher gap heights. Hence, generation of turbulent kinetic energy during flow through the micro gap decreases. However, after 2 mm of micro gap height, the effect of further gap height increment on turbulent kinetic energy generation is small.

Similar effect has also been observed for fin spacing. In Figure-5., it is found that turbulent kinetic energy descends almost linearly with the increment of fin spacing. While fin spacing increases, cross-sectional area of the micro gap increases as well. It results lower pressure drop inside the gap during flow. As a result, turbulent kinetic energy decreases.

ISSN 1819-6608
ARPN Journal of Engineering and Applied Sciences

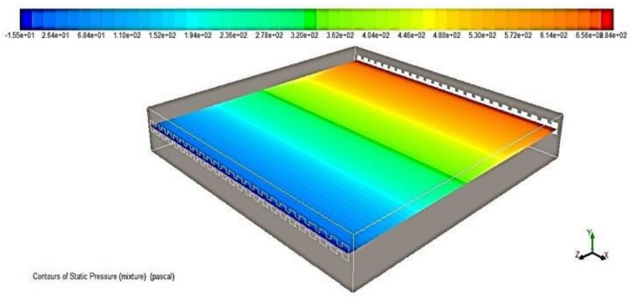

(a)

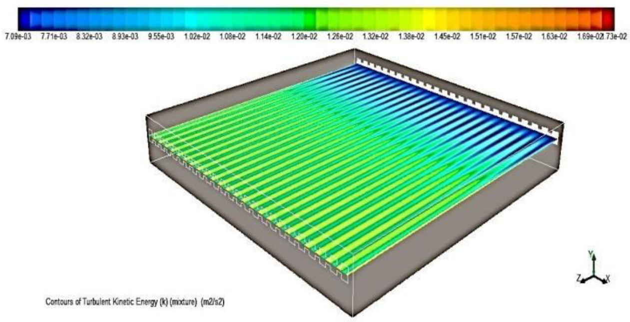

(b)

Figure-2. Pressure distribution (a) and turbulent kinetic energy distribution (b) on X-Z plan at Y=2.5 mm for surface roughness 0.05 mm.

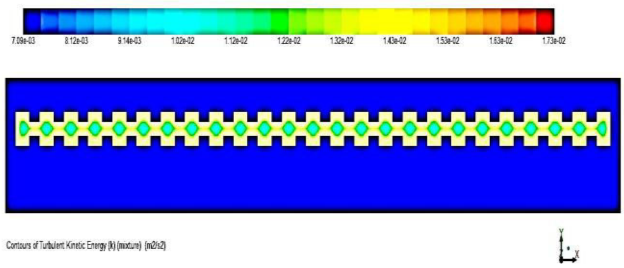

Figure-3. Turbulent kinetic energy distribution on X-Y plan at Z=15 mm for surface roughness 0.05 mm.

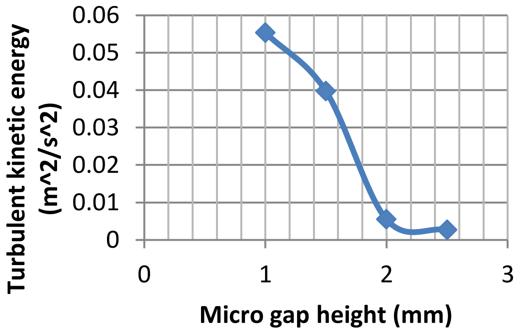

Figure-4. Turbulent kinetic energy vs. micro gap height for $\dot{m} = 0.059$ kg/s.

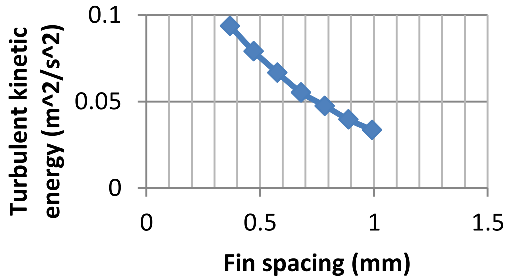

Figure-5. Turbulent kinetic energy vs. fin spacing for$\dot{m} = 0.059$ kg/s.

Effect of surface roughness

From Figure-6., it is observed that for 2mm of gap height, turbulent kinetic energy is almost invariant with the increment of surface roughness height from 0.01-0.03 mm, while Reynolds number at the inlet is Re = 1100. After that k increases linearly with further increment of surface roughness. This is because after 0.03 mm of roughness height, friction coefficient increases with surface roughness increment. However, for 1 mm of gap height, k remains unchanged until 0.04 mm of roughness height and slightly increases for 0.05 mm. It is seen that increment rate of turbulent kinetic energy in micro gap of 2 mm height is much higher than 1mm gap height.

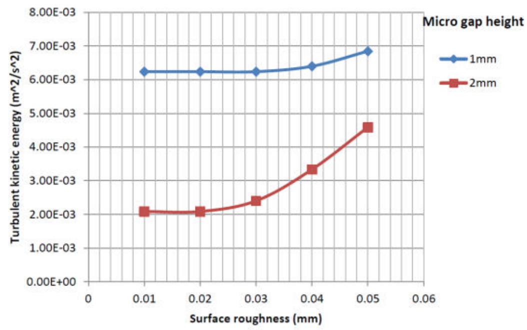

Figure-6. Turbulent kinetic energy vs. surface roughness for Re = 1100.

CONCLUSIONS

Turbulent kinetic energy generation under various conditions in a micro finned micro gap has been investigated by numerical simulation. However, only steady-state analysis has been done. A transient analysis should be carried out further as it may provide better results.

From results, it has been perceived that turbulent kinetic energy is influenced by pressure drop. By increasing micro gap height, pressure drop decreases. As a result, generation of turbulent kinetic energy also decreases. However, effect of micro gap height on turbulent kinetic energy decreases after 2 mm of gap height. Generation of turbulent kinetic energy decreases linearly with the increment of fin spacing. Effect of surface roughness on turbulent kinetic energy generation is also influenced by micro gap height. Turbulent kinetic energy is more sensitive to surface roughness in higher gap heights.

ACKNOWLEDGEMENT

The support of the Ministry of Education, Malaysia under the grant FRGS 13-020-0261 is gratefully acknowledged. This research was also supported by International Islamic University Malaysia from Endowment Type B fund (EDW B14-127-1012).

REFERENCES

[1] Tuckerman B. and Pease R. F. W. 1981. High-performance heat sinking for VLSI. Electron Device Letters, IEEE 2.5. pp. 126 –129.

[2] Alam T., Lee P. S., Yap C. R. and Jin L. W. 2011. Experimental investigation of microgap cooling technology for minimizing temperature gradient and mitigating hotspots in electronic devices. 13th Electronics Packaging Technology Conference (EPTC). pp. 530-535.

[3] Stehlík P., Jegla Z. and Kilkovský B. 2014. Possibilities of intensifying heat transfer through finned surfaces in heat exchangers for high temperature applications. Applied Thermal Engineering. 70(2): 1283-1287.

[4] Nguyen N.T., Bochnia D., Kiehnscherrf R. and Dözel W. (1996). Investigation of forced convection in microfluid systems, Sensors Actuators A. 55: 49-55.

[5] Seder I. M., Ahmed M. I., Ahmed S. and Hawlader, M. N. A. 2014. Feasibility of double-layer microchannel fabrication at low speed micro end-mill and wire-cut EDM machines. Australian Journal of Basic and Applied Sciences. 8(15): 211-217.

[6] Wu P. and Little W.A. 1983. Measurement of friction factors for the flow of gases in very fine channels used for microminiature Joule-Thompson refrigerators, Cryogenics 23: 273-277.

[7] Mirzabeygi P. and Zhang C. 2015. Turbulence modeling for the two-phase flow and heat transfer in condensers. International Journal of Heat and Mass Transfer. 89: 229-241.

[8] Zhang R., Cong T., Tian W., Qiu S. and Su G. 2015. Effects of turbulence models on forced convection subcooled boiling in vertical pipe. Annals of Nuclear Energy. 80: 293-302.

[9] Vlahostergios Z., Missirlis D., Flouros M., Albanakis C. and Yakinthos K. 2015. Effect of turbulence intensity on the pressure drop and heat transfer in a staggered tube bundle heat exchanger. Experimental Thermal and Fluid Science. 60: 75-82.

[10] Abid M., Noon A. A. and Wajid H. A. 2010. Simulation of turbulent flow through tarbela dam tunnel 3. IIUM Engineering Journal. 11(2): 201-224.

[11] Kelvin H.C.S., Yousif A.A. and Andrew C. 2012. Unsteady heat transfer in an annular pipe, Part II: swirling laminar flow. IIUM Engineering Journal. 12(6): 79-95.

[12] Hirt C. W. and Nichols B. D. 1981. Volume of fluid (VOF) method for the dynamics of free boundaries. Journal of Computational Physics. 39(1): 201–225.

[13] Lee W. H. 1979. A Pressure Iteration Scheme for Two-Phase Modeling, Technical Report LA-UR. Los Alamos Scientific Laboratory, Los Alamos, New Mexico. pp. 79-975.

[14] Wu H. L., Peng X. F., Ye P. and Gong Y. E. 2007. Simulation of Refrigerant Flow Boiling in Serpentine Tubes. International Journal of Heat and Mass Transfer. 50(5): 1186–1195.

[15] De Schepper, S. C., Heynderickx G. J. and Marin G. B. 2009. Modeling the Evaporation of a Hydrocarbon Feedstock in the Convection Section of a Steam Cracker. Computers and Chemical Engineering. 33(1): 122-132.

[16] Alizadehdakhel A., Rahimi M. and Alsairafi A. A. (2010). CFD Modeling of Flow and Heat Transfer in a Thermosyphon. International Communications in Heat and Mass Transfer. 37(3): 312–318.

[17] Orszag S. A., Yakhot V., Flannery W. S., Boysan F., Choudhury D., Maruzewski J. and Patel B. 1993. Renormalization Group Modeling and Turbulence Simulations. International Conference on Near-Wall Turbulent Flows, Tempe, Arizona. 1031-1046.

[18] Patankar S. V. and Spalding, D. B. 1972. A calculation procedure for heat, mass and momentum transfer in three-dimensional parabolic flows. International Journal of Heat and Mass Transfer. 15(10): 1787-1806.